Available online at www.sciencedirect.com
ScienceDirect
Journal of Sound and Vibration 297 (2006) 680–693
JOURNAL OF SOUND AND VIBRATION
www.elsevier.com/locate/jsvi

Vibration control of piezoelectric smart structures based on system identification technique: Numerical simulation and experimental study

Xing-Jian Dong*, Guang Meng, Juan-Chun Peng

State Key Laboratory of Vibration, Shock and Noise, Shanghai JiaoTong University, Shanghai, 200030, People's Republic of China

Received 26 July 2004; received in revised form 12 April 2006; accepted 17 April 2006
Available online 23 June 2006

Abstract

The aim of this study is to investigate the efficiency of a system identification technique known as observer/Kalman filter identification (OKID) technique in the numerical simulation and experimental study of active vibration control of piezoelectric smart structures. Based on the structure responses determined by finite element method, an explicit state space model of the equivalent linear system is developed by employing OKID approach. The linear quadratic Gaussian (LQG) algorithm is employed for controller design. The control law is then incorporated into the ANSYS finite element model to perform closed loop simulations. Therefore, the control law performance can be evaluated in the context of a finite element environment. Furthermore, a complete active vibration control system comprising the cantilever plate, the piezoelectric actuators, the accelerometers and the digital signal processor (DSP) board is set up to conduct the experimental investigation. A state space model characterizing the dynamics of the physical system is developed from experimental results using OKID approach for the purpose of control law design. The controller is then implemented by using a floating point TMS320VC33 DSP. Numerical examples by employing the proposed numerical simulation method, together with the experimental results obtained by using the active vibration control system, have demonstrated the validity and efficiency of OKID method in application of active vibration control of piezoelectric smart structures.
© 2006 Elsevier Ltd. All rights reserved.

1. Introduction

A smart structure used in vibration control can be defined as a structure or structure component with bonded or embedded sensors and actuators as well as an associated control system, which enables the structure to respond simultaneously to external stimuli exerted on it and then suppresses undesired effects or enhance desired effects [1]. It involves multi-discipline knowledge, such as mechanics, mechanical engineering, modern control theory, and computer science. The performance requirements of future space structures, jet fighters and concept automobiles have brought much interest to the area of smart structures.

Piezoelectric materials, such as lead zirconate titanate (PZT), produce an electric field when deformed and undergo deformation when subjected to an electric field. Owing to this intrinsic coupling phenomenon,

*Corresponding author. Tel.: +86 21 54744990; fax: +86 21 54747451.
E-mail address: donxij@hotmail.com (X.-J. Dong).

0022-460X/$ - see front matter © 2006 Elsevier Ltd. All rights reserved.
doi:10.1016/j.jsv.2006.04.021

piezoelectric materials are widely used as sensors and actuators in smart structures. Among various smart structures, those with piezoelectric patches have received much attention in recent years, due to the fact that piezoelectric materials have simple mechanical properties, small volume, light weight, large useful bandwidth, efficient conversion between electrical and mechanical energy, good ability to perform vibration control and ease of integration into metallic and composite structures [2,3]. The technology of piezoelectric smart structures has become mature over the last decade [4].

To design piezoelectric smart structures for active vibration control, both structural dynamics and control theory need to be considered. The finite element method, a widely accepted and powerful tool for analyzing complex structures, is capable of dealing with the piezoelectric smart structures. Numerous studies have been completed on analyzing piezoelectric structures. Special finite elements have been developed to account for piezoelectric effect [5–7]. Among commercially available finite element analysis (FEA) codes, ANSYS, has the ability to model piezoelectric materials. Based on the finite method model, the mode superposition technique is widely used to transform the coupled finite element equations of motion in the physical coordinates into a set of reduced uncoupled equations in the modal coordinates, and then the state space model of the system is developed [1,8,9]. Commonly, the MatLAB Control System Toolbox is used for the control law design and then closed loop simulation is performed based on the state space model of reduced order [8,10]. As can be seen, in most of the present researches, if not all, dynamic modeling of the smart structures and design of the control systems are usually carried out separately without taking the interaction between the structure and the control system into account. Due to the increasing interest in the design of complex piezoelectric smart structures and the need for fast and simple implementation of piezoelectric control systems, it is necessary to develop a general design scheme of actively controlled piezoelectric smart structures and then experimentally study the efficiency of the control law.

In this study, a modern system identification technique is employed to develop an explicit state space model for control law design from the output of a commercial finite element code ANSYS. System identification technique stems from control engineering, which is widely employed to develop a mathematical model given experiment data for the purpose of control law design. This requires the construction of a minimum order model from the test data that characterizes the dynamics of the system at the selected control and measurement positions. A finite element simulation provides time histories of the variables of a piezoelectric smart structure, but does not generate an explicit mathematical model of the system. Finite element simulations are analogous to performing experimental investigations where the only direct outputs are time responses. Therefore, the structural responses determined by finite element simulations are employed as the inputs to an identification technique known as observer/Kalman filter identification (OKID) [11,12] approach that identifies the Markov parameters of an asymptotically stable observer. The system Markov parameters are then determined recursively from the Markov parameters of the observer system, from which a state space realization is obtained using the eigensystem realization algorithm (ERA) [11,13]. A linear quadratic gaussian (LQG) based robust controller which is less insensitive to system parameter variations, and also works efficiently when multiple modes of vibration are present in the response, is employed to design a control law for controlling the vibrations of the piezoelectric smart structures. ANSYS parametric design language (APDL) is then used to integrate the control law into the ANSYS finite element model to perform closed loop simulations.

The goals of this research are to propose a general analysis and design scheme of piezoelectric smart structures by using ANSYS and OKID approach, and to experimentally study the feasibility and efficiency of OKID approach in the vibration control of piezoelectric smart structures. The experimental object of this research is comprised of a cantilever plate, piezoelectric actuators, accelerometers and digital signal processor (DSP) board. The rest of the paper is organized into four sections. In Section 2, based on the finite element model of a piezoelectric smart structure, an explicit state space model of the equivalent linear system is developed for the purpose of control law design. The OKID approach is summarized in brief. In Section 3, the LQG control law design technique is employed to design a control law. By using APDL, the control law is then incorporated into the ANSYS finite element model to perform closed loop simulations. In Section 4, numerical examples are presented to demonstrate the validity of the proposed design scheme. And then a complete active vibration control system is set up to conduct experimental investigation. Section 5 concludes the study.

2. Control design model development

2.1. Finite element model

It is assumed that the thermal effect is not considered in the analysis. The linear piezoelectric coupling between the elastic field and the electric field can be expressed by the direct and the converse piezoelectric equations respectively [14]

$$\{D\} = [e]\{\varepsilon\} + [\bar{\varepsilon}]\{E\}, \tag{1}$$

$$\{\sigma\} = [Q]\{\varepsilon\} - [e]^{\mathrm{T}}\{E\}, \tag{2}$$

where electrical variable $\{D\}$ and $\{E\}$ denote the electric displacement and the electric field intensity, respectively; mechanical variables $\{\sigma\}$ and $\{\varepsilon\}$ denote the stress and the strain, respectively. Matrices $[Q]$, $[e]$ and $[\bar{\varepsilon}]$ represent material properties: $[Q]$ is the elastic stiffness matrix, $[e]$ is the piezoelectric stress coefficient matrix, and $[\bar{\varepsilon}]$ is the permittivity matrix. The superscript "T" denotes the transpose of a vector or matrix.

Modeling of piezoelectric smart structures by the finite element method and its implementation for active vibration control problems have been presented in Ref. [5–8,15,16]. The global matrix equations governing a smart structure system can be written as

$$\begin{bmatrix} M_{uu} & 0 \\ 0 & 0 \end{bmatrix} \begin{Bmatrix} \ddot{u} \\ \ddot{\phi} \end{Bmatrix} + \begin{bmatrix} C_{uu} & 0 \\ 0 & 0 \end{bmatrix} \begin{Bmatrix} \dot{u} \\ \dot{\phi} \end{Bmatrix} + \begin{bmatrix} K_{uu} & K_{u\phi} \\ K_{u\phi}^{\mathrm{T}} & K_{\phi\phi} \end{bmatrix} \begin{Bmatrix} u \\ \phi \end{Bmatrix} = \begin{Bmatrix} F_u \\ F_\phi \end{Bmatrix}, \tag{3}$$

where u denotes structural displacement, ϕ denotes electric potential, and a dot above a variable denotes a time derivative; F_u denotes the structural load and F_ϕ denotes the electric load; M_{uu} and K_{uu} are the structural mass and stiffness matrix, respectively, $K_{u\phi}$ is the piezoelectric coupling matrix and $K_{\phi\phi}$ is the dielectric stiffness matrix, C_{uu} is the damping matrix, which is usually assumed to be a linear combination of the structural mass matrix M_{uu} and the structural matrix K_{uu}

$$[C_{uu}] = \alpha[M_{uu}] + \beta[K_{uu}]. \tag{4}$$

The constants α and β are the damping parameters [17]. It is notable to point out that proportional damping is assumed but not required for system identification.

As mentioned before, the commercial finite element code ANSYS can be utilized to model the piezoelectric smart structure with prescribed inputs to obtain a set of corresponding output time histories. The next step is to employ a system identification technique, using the time histories of outputs and inputs of the ANSYS finite element model, to determine an "equivalent linear system" for use as a control law design model.

2.2. Description of observer/Kalman filter identification technique

The OKID [11,12] method was developed to compute the Markov parameters of a linear system, which are the same as its pulse response samples. The OKID technique has been applied to space structures, such as the Shuttle Remote Manipulator system [18]. The method is formulated entirely in the time domain, and is capable of handling general response data. One of the keys to the OKID algorithm is the introduction of an observer into the identification process. The first step of the process is the calculation of the observer Markov parameters. Then the system Markov parameters are determined recursively from the Markov parameters of the observer system. In the following we will summarize it in brief.

Firstly, consider a general discrete multivariable linear system expressed in the state space format

$$\begin{aligned} x(i+1) &= Ax(i) + Bu(i), \\ y(i) &= Cx(i) + Du(i), \end{aligned} \tag{5}$$

where x is an $n \times 1$ state vector, u an $m \times 1$ input or control vector, y a $q \times 1$ output vector. Matrices A, B, C and D are the state matrix, input matrix, output matrix, and direct influence matrix, respectively. The integer i is the sample indicator. The input–output description of the above system with zero initial conditions can be obtained from Eq. (5) recursively as

$$y(i) = \sum_{\tau=0}^{i-1} Y_\tau u(i-\tau-1) + Du(i), \tag{6}$$

where the parameters

$$Y_\tau = CA^\tau B$$

together with D, are known as the Markov parameters of the system, which are also the system pulse response samples. To reduce the number of Markov parameters needed to adequately model a system, an observer is introduced into the OKID technique. If (A, C) is an observable pair, then there exists an observer of the form

$$\begin{aligned} \widehat{x}(i+1) &= A\widehat{x}(i) + Bu(i) - M[y(i) - \widehat{y}(i)] \\ &= (A+MC)\widehat{x}(i) + (B+MD)u(i) - My(i), \\ \hat{y}(i) &= C\widehat{x}(i) + Du(i). \end{aligned} \tag{7}$$

The matrix M can be interpreted as an observer gain. Consider the special case where M is a deadbeat observer gain such that all eigenvalues of $A+MC$ are zero, the estimated state $\hat{x}$ converges to the true state $x(i)$ after at most n steps where n is the order of the system. Eq. (7) then becomes

$$\begin{aligned} x(i+1) &= (A+MC)x(i) + (B+MD)u(i) - My(i), \\ y(i) &= Cx(i) + Du(i). \end{aligned} \tag{8}$$

The input–output description of the system in Eq. (8) is

$$y(i) = \sum_{\tau=0}^{n-1} \bar{Y}_\tau [\, u(i-\tau-1) \quad y(i-\tau-1)\,]^{\mathrm{T}} + Du(i) \quad i \geq n, \tag{9}$$

where

$$\begin{aligned} \bar{Y}_\tau &= [C(A+MC)^\tau(B+MD) - C(A+MC)^\tau M] \\ &= [\bar{Y}_\tau^{(1)}\,\bar{Y}_\tau^{(2)}]. \end{aligned}$$

$\bar{Y}_\tau$ and D are the Markov parameters of an observer system. A particular feature of the deadbeat observer is that the Markov parameters $\bar{Y}_\tau$ will become identically zero after a finite number of time steps. The standard recursive least-squares technique is used to solve Eq. (9) and then the observer Markov parameters are computed. There is an algebraic relationship between the Markov parameters of the observer system and those of the actual system

$$Y_\tau = CA^\tau B = \bar{Y}_\tau^{(1)} + \sum_{i=0}^{\tau-1} \bar{Y}_i^{(2)} Y_{\tau-i-1} + \bar{Y}_\tau^{(2)} D. \tag{10}$$

A complete description for the computation of the Markov parameters is given in Refs. [11,12,19]. Once the Markov parameters of the observer system are identified, the actual system Markov parameters can be recovered according to Eq. (10). The actual system Markov parameters are then used to obtain a state space model of the system by a realization procedure called the ERA [11,13].

2.3. *Minimum realization by the eigensystem realization algorithm*

The ERA is a system realization method that has been studied extensively [11,13]. It determines a state space model (A_r, B_r, C_r, D_r) of a structure from the system Markov parameters. The algorithm begins by forming the

$l \times l$ block Hankel matrix denoted by $H(l, \tau)$

$$H(l,\tau) = \begin{bmatrix} Y_\tau & Y_{\tau+1} & \cdots & Y_{\tau+l-1} \\ Y_{\tau+1} & Y_{\tau+2} & \cdots & Y_{\tau+l} \\ \vdots & \vdots & & \vdots \\ Y_{\tau+l-1} & Y_{\tau+l} & \cdots & Y_{\tau+2l-2} \end{bmatrix}. \tag{11}$$

The order of the system is determined from the singular value decomposition of $H(l,0)$

$$H(l,0) = U\Sigma V^{\mathrm{T}}, \tag{12}$$

where the matrix U and V are unitary matrices, Σ is an $n \times n$ diagonal matrix of positive singular values, and n is the order of the system. Defining a $q \times lq$ matrix E_q^{T} and an $m \times lm$ matrix E_m^{T} made up of identity and null matrices of the form

$$E_q^{\mathrm{T}} = [I_q 0_{q\times(l-1)q}], \quad E_m^{\mathrm{T}} = [I_m 0_{m\times(l-1)m}] \tag{13}$$

a discrete-time minimal order realization of the system can be written as

$$A_r = \Sigma^{-1/2} U^{\mathrm{T}} H(l,1) V \Sigma^{-1/2}, \tag{14a}$$

$$B_r = \Sigma^{1/2} V^{\mathrm{T}} E_m, \tag{14b}$$

$$C_r = E_q^{\mathrm{T}} U \Sigma^{1/2}. \tag{14c}$$

The direct influence matrix D_r can be identified by solving Eq. (9). The above state space model of the system dynamics is used to design a LQG-based robust controller.

3. Control algorithm and closed loop simulation

3.1. LQG design

The robust controller design using the LQG is discussed in this section. Considering the process and measurement noise $w(i)$ and $v(i)$, the state space equation for the piezoelectric smart structure can be written as

$$\begin{aligned} x(i+1) &= A_r x(i) + B_r u(i) + G w(i), \\ y(i) &= C_r x(i) + D_r u(i) + v(i). \end{aligned} \tag{15}$$

In the LQG algorithm, the process noise $w(i)$ and the measurement noise $v(i)$ are both assumed to be stationary, zero-mean, Gaussian white, and have covariance matrices satisfying

$$\begin{aligned} \mathrm{Cov}\{w(i), w(j)\} &= E\{w(i)w^{\mathrm{T}}(j)\} = V_{1,ii}\delta_{i,j}, \\ \mathrm{Cov}\{v(i), v(j)\} &= E\{v(i)v^{\mathrm{T}}(j)\} = V_{2,ii}\delta_{i,j}, \end{aligned} \tag{16}$$

where $\mathrm{E}\{\cdot\}$ denotes the expected value, $\delta_{i,j}$ denotes the Kronecker delta, V_1 and V_2 are both diagonal matrices. In addition, $w(i)$ and $v(i)$ are assumed to be uncorrelated. The controller consists of a state feedback module and a state estimation module. The former corresponds to the following control law:

$$u(i) = -Kx(i) \tag{17}$$

in which K denotes the feedback gain matrix. The feedback gain matrix is obtained so as to minimize the quadratic cost function of the form

$$J = E\left\{\sum_{i=1}^{\infty}[x^{\mathrm{T}}(i)Qx(i) + u^{\mathrm{T}}(i)Ru(i)]\right\}, \tag{18}$$

where Q is a symmetric positive semi-definite matrix and R is a symmetric positive-definite matrix. The optimal feedback gain matrix that minimizes the above cost function is given by

$$K = (R + B_r^{\mathrm{T}}P_1B_r)^{-1}B_r^{\mathrm{T}}P_1A_r, \tag{19}$$

where the positive definite matrix P_1 is the solution to the following algebraic Riccati equation

$$A_r^{\mathrm{T}}P_1A_r - P_1 - A_r^{\mathrm{T}}P_1B_r(R + B_r^{\mathrm{T}}P_1B_r)^{-1}B_r^{\mathrm{T}}P_1A_r + Q = 0. \tag{20}$$

In Eq. (17) it is assumed that all of the states are available for feedback. However, in practice only the system outputs are available for feedback. To estimate the states of the system from sensor outputs, a state estimator based on the Kalman filter is designed

$$\widehat{x}(i+1) = A_r\widehat{x}(i) + B_ru(i) + L[y(i) - C_r\hat{x}(i) - D_ru(i)], \tag{21}$$

where $\hat{x}(i)$ denotes the estimated state and the observer gain matrix is obtained form

$$L = A_rP_2C_r^{\mathrm{T}}(C_rP_2C_r^{\mathrm{T}} + V_2)^{-1} \tag{22}$$

in which the positive P_2 satisfies the following algebraic Riccati equation

$$A_r^{\mathrm{T}}P_2A_r + GV_1G^{\mathrm{T}} - A_rP_2C_r^{\mathrm{T}}(C_rP_2C_r^{\mathrm{T}} + V_2)^{-1}C_rP_2A_r^{\mathrm{T}} - P_2 = 0. \tag{23}$$

Note that the state vector in Eq. (17) should be replaced by the estimated state $\hat{x}(i)$. One of the merits of the LQG technique lies in the separation principle, which states that the design of the feedback and the estimator can be carried out separately. A block diagram of the LQG controller is shown in Fig. 1.

The selection of Q and R is vital in the control design process. Q and R are the free parameters of design and stipulate the relative importance of the control result and the control effort. A large Q puts higher demand on control result, and a large R puts more limits on control effort [20]. The optimal values for Q and R are typically obtained by trial-and-error methods. An efficient way of choosing Q is to compute it from C_r with

$$Q = C_r^{\mathrm{T}}C_r. \tag{24}$$

Weighting matrix R can be set as ρI with ρ as a scalar design parameter. Therefore, the challenging task of choosing Q and R reduces to choosing one parameter ρ. Consequently, the control performance such as

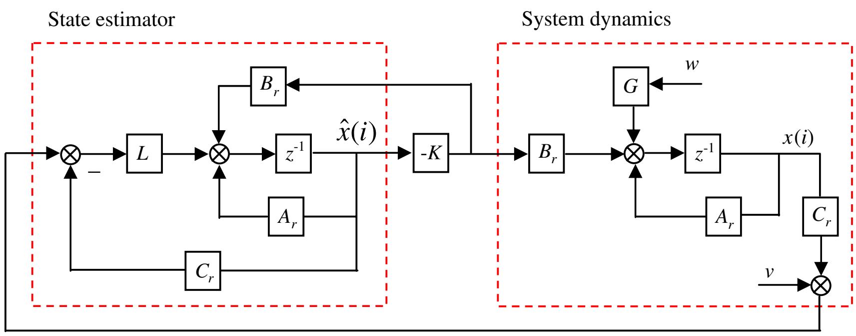

Fig. 1. A block diagram of the discrete-time LQG controller.

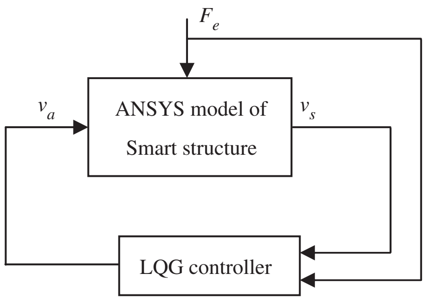

Fig. 2. Block diagram of the closed loop simulation.

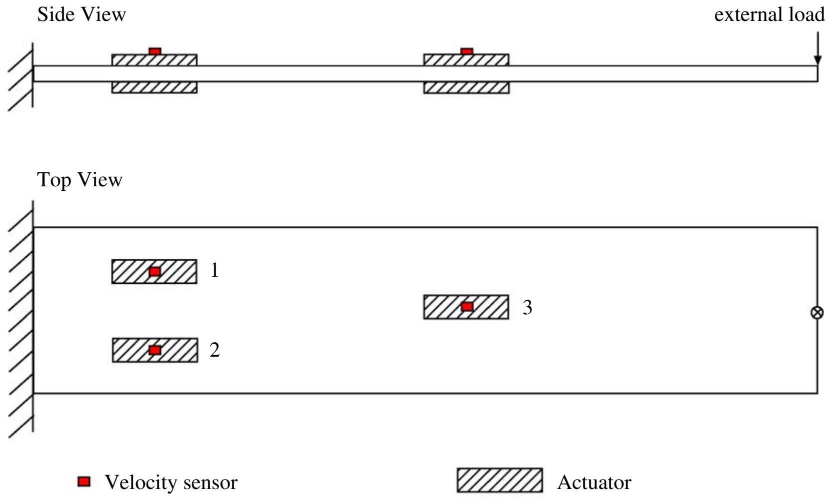

Fig. 3. The configuration of an actively controlled cantilever plate.

settling time and the maximum value of the actuator voltage can be tuned through changing the value of ρ. This procedure is used in the illustrative example presented next.

3.2. Closed loop simulation in finite element environment

As discussed earlier, finite element simulations are analogous to performing experimental investigations. In this section, by using APDL, the ANSYS finite element model of a smart structure is modified to accept control laws and perform closed loop simulations. Therefore, the control law can be evaluated in the context of finite element environment. The block diagram of the analysis is shown in Fig. 2. F_e is the vibration generating force. The instantaneous value of the vibration generating force is defined at each time step. $\boldsymbol{v}_s$ is the sensor signal at a sensor location. For instance, for a cantilever plate, vertical velocity can serve as sensor signal. $\boldsymbol{v}_a$ is the actuator voltage and it is determined by the LQG controller using F_e and $\boldsymbol{v}_s$.

In this study, to construct an ANSYS finite element model for a piezoelectric smart structure, SOLID45 elements are used for the metal part and SOLID5 elements are used for the piezoelectric part of the structure. A macro has been written to perform the transient analysis, in which the control law is accepted. In the transient analysis, the instantaneous value of the sensor signal is calculated at a time step. Then the feedback voltage, which will be used as the input to the piezoelectric actuator during the next time step, is determined by the LQG controller. This process will continue for the predefined time duration of the computed response. Through the results of transient analysis, the control law can be evaluated in the finite element simulation.

If the control law performance is not adequate, the control law can be redesigned and evaluated again until the desired performance is obtained.

4. Numerical examples and experimental investigation

4.1. Numerical examples

In this section, a cantilevered plate is considered. The structure consists of a host aluminum plate ($700\,\text{mm} \times 150\,\text{mm} \times 1.2\,\text{mm}$), APC-850 piezoelectric patches ($70\,\text{mm} \times 15\,\text{mm} \times 0.5\,\text{mm}$) and velocity sensors. The adhesive layers are neglected. The piezoelectric patches work as actuators are perfectly bonded on the upper and lower surfaces of the plate structure at the same location. It is assumed that the same magnitude but the opposite direction of electric field is applied to the upper and lower piezoelectric patches so as to create a pure bending moment for vibration suppression. Velocity sensors are bonded on top of the actuators. The configuration of the structure is shown in Fig. 3. As can be seen in Fig. 3, there are three

Table 1
Material properties of APC850 and aluminum

—	APC850	Al
E_{11} (GPa)	63.0	69.0
E_{22} (GPa)	63.0	69.0
E_{33} (GPa)	54.0	69.0
G_{12} (GPa)	24.6	27.0
G_{23} (GPa)	24.6	27.0
G_{13} (GPa)	30.6	27.0
ν_{12}	0.35	0.32
ν_{23}	0.44	0.32
ν_{13}	0.38	0.32
d_{31} (m/V)	-1.75×10^{-10}	/
d_{33} (m/V)	4.00×10^{-10}	/
d_{15} (m/V)	5.90×10^{-10}	/
$\bar{\varepsilon}_{11}$ (F/m)	1.43×10^{-8}	/
$\bar{\varepsilon}_{33}$ (F/m)	1.55×10^{-8}	/
ρ (kg/m^3)	7600.0	2700.0

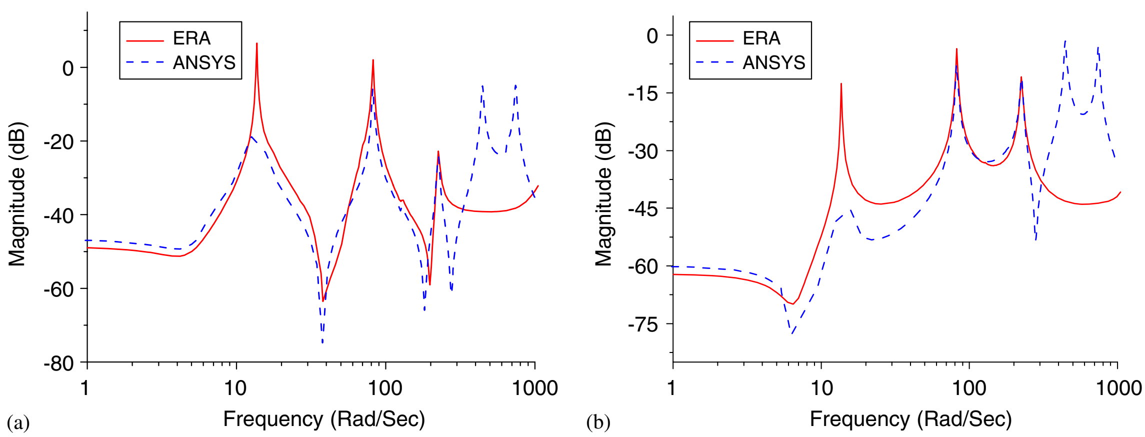

Fig. 4. Frequency response functions: (a) from actuator 1 to sensor 3; (b) from actuator 3 to sensor 2.

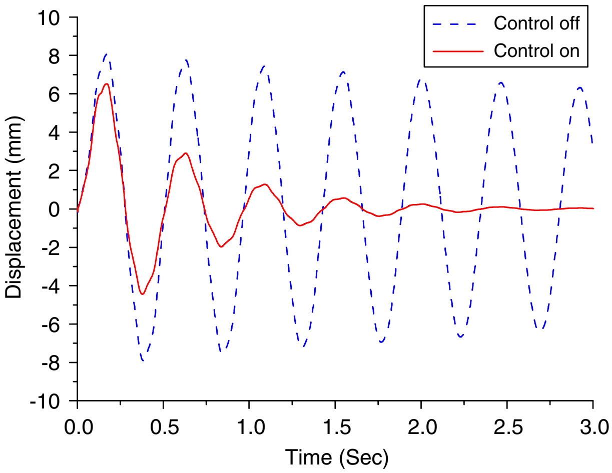

Fig. 5. Displacement response to impulse excitation.

actuator pairs marked with actuator 1, actuator 2 and actuator 3, respectively. Also, there are three sensors marked with sensor 1, sensor 2 and sensor 3, respectively. It should be pointed out that in ANSYS finite element model the elastic and inertial properties of the sensors are not taken into account. The first 10 modes are taken into account to perform mode modal transient response analysis. Uniform damping ratio of 1.0% is used except 0.8% for the first mode. The transverse velocities at sensor locations are calculated at each time step and then serve as sensor signals. The material properties of APC850 and aluminum are listed in Table 1.

White noise is selected as the input signal since it satisfies the condition of persistent excitation, as required by a reliable identification [21]. Finite element simulation using ANSYS is performed to obtain a set of corresponding output time histories. The aforementioned system identification technique is then employed, using the time histories of inputs and outputs, to set up a state space model for use as a control law design model. Frequency response functions can be obtained from the state space model. For brevity, only two of them are shown in Fig. 4. The results from the ANSYS finite element model are also shown in Fig. 4 for the purpose of comparison. Fairly good agreement is observed between the two results except for the frequency range above 300 rad/sec. For most structure systems under practical loading conditions, only the first few modes play important parts in the vibration response of the system. Therefore, it can be concluded that the state space model developed by identification technique characterizes the dynamics of the system and can be used for control law design.

For the LQG controller, the free parameters ρ, V_1 and V_2 are selected as $\rho = 0.001$, $V_1 = 10^{-3} I_n$ and $V_2 = 10^{-6} I_q$. As mentioned previously, these parameters are determined by trial-and-error methods to most effectively control the structure. At the same time, these parameters are limited for the sake of the breakdown voltage of the piezoelectric materials. The maximum voltage per thickness of the piezoelectric material is taken as $300\,\mathrm{V\,mm^{-1}}$. Once the LQG controller design is completed, APDL is used to integrate control law into the ANSYS finite element model to perform closed loop simulations. Finally, the control law is evaluated in the finite element simulation. If the control law performance is not adequate, the control law can be redesigned and reevaluated until the desired performance is obtained.

The external load is assumed to be applied at the free end of the plate and the dynamic responses at the free end, i.e. the tip displacements, are given to evaluate the control law. For case 1, a transverse impulsive loading of 0.1 N is applied at the free end of the plate for 0.1 s. Transient responses of the plate tip displacement are shown in Fig. 5. Results when the control is off are also shown for comparison. Actuator voltages are shown in Fig. 6. As can be seen, the controller successfully damps the vibration of the plate. The actuator voltages are lower than the breakdown voltage of piezoelectric materials. For case 2, banded limited white noise in the frequency range 0–200 rad/s is applied at the free end of the plate. The tip displacement of the plate and the actuator voltages are shown in Figs. 7 and 8, respectively. The controller is also effective in controlling the random vibration. Still, the actuator voltages are lower than the breakdown voltage of piezoelectric materials.

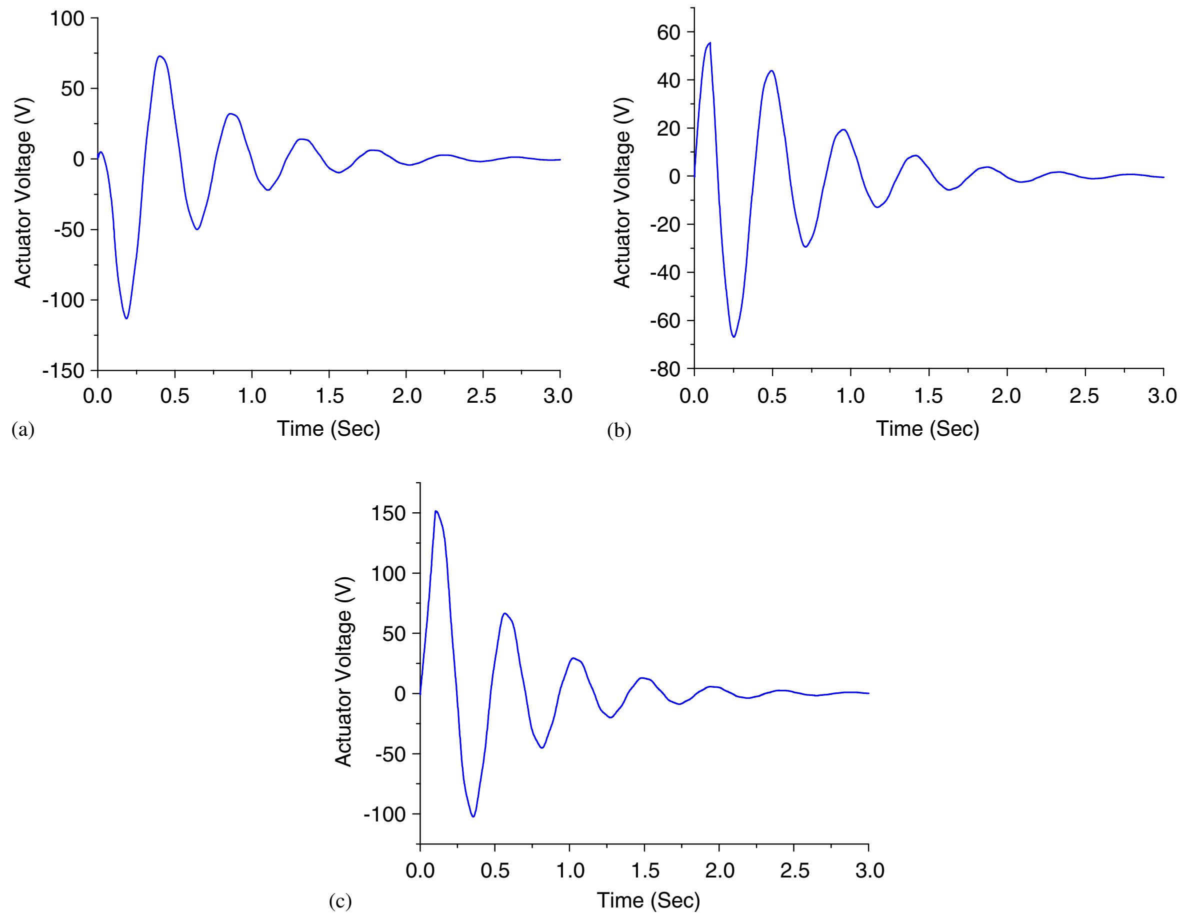

Fig. 6. Time histories of actuator voltage for case 1: (a) actuator 1; (b) actuator 2; (c) actuator 3.

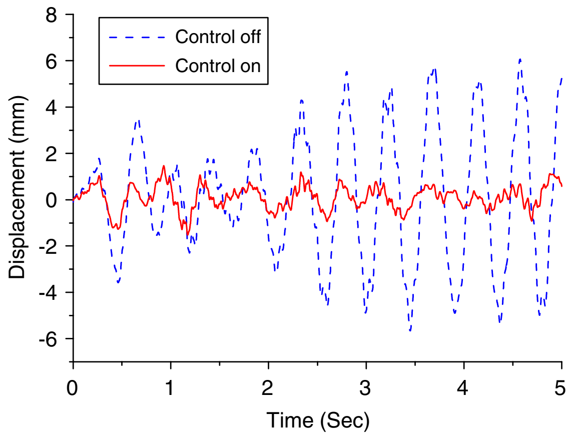

Fig. 7. Displacement response to random excitation.

4.2. *Experimental investigation*

In this section, we shall experimentally evaluate the effectiveness of the proposed identification technique in the vibration control of piezoelectric smart structures. The piezoelectric structure considered in experimental

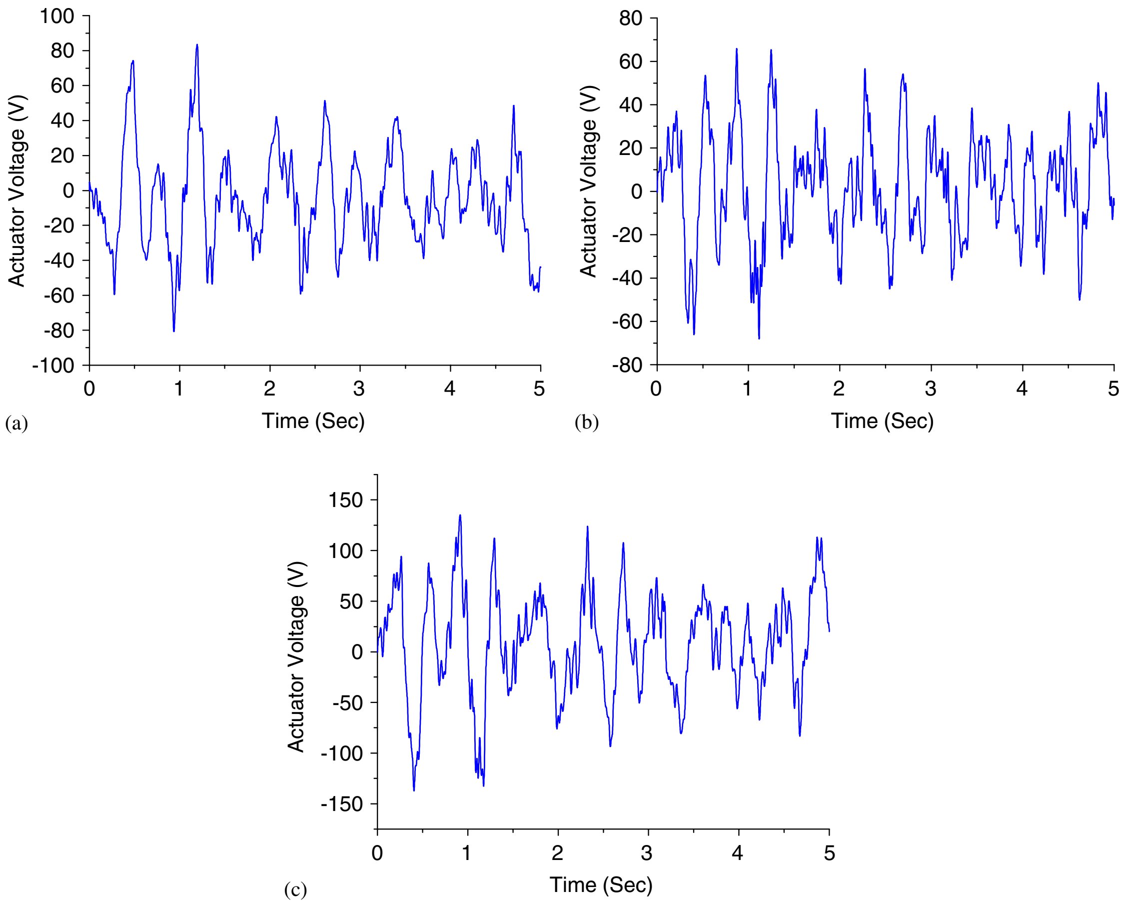

Fig. 8. Time histories of actuator voltage for case 2: (a) actuator 1; (b) actuator 2; (c) actuator 3.

investigation is shown in Fig 9. Note that accelerometers are used as sensors in this structure. The test structure is not exactly the same as the one used in simulation described in Section 4.1. The dimension of the rectangular aluminum plate is 500 mm × 70 mm × 1.2 mm. The used piezoelectric patch is APC-850 and its dimension is 70 mm × 15 mm × 0.5 mm. Three piezoelectric patches, denoted as actuator 1–actuator 3, are bonded on the lower surface as actuators. Three accelerometers, denoted as sensor 1–sensor 3, collocated on the upper surface as sensors. The distance between the left end of the actuator 1 and the clamped end of the plate is 10 mm, and that of the actuator 3 is 210 mm. The inputs of the system are the voltages applied to the piezoelectric actuators and the outputs of the system are the acceleration signals. The inputs and outputs are both electrical signals that can easily be measured by a dynamic signal analyzer.

Fig. 10 depicts the experimental setup. The 16-channel DATA PHYSICS SignalCalc430 dynamic signal analyzer is used for generating, analyzing and storing signals. The three-channel high voltage power amplifier (HIT BoShi Precision Measure & Control Co., China), capable of driving highly capacitive loads, is used to supply necessary voltages for the actuating piezoelectric patches. The Polytec OFV-3000 laser vibrometer is used to monitor the vibration of the plate at the free end. The controller is implemented using a multi-channel and multifunctional DSP board consisting of D/A and A/D interfaces, anti-alias filters, smoothing filters and a TMS320VC33 DSP. The sampling rate is chosen to be 1 kHz, which gives an effective control bandwidth of 200 Hz. This bandwidth includes the four lowest modes of the structure (see Table 2).

Single input multi output tests are conducted for the purpose of identifying the physical system. Pseudo random signal generated by the signal analyzer is applied to each piezoelectric patch through the voltage power amplifier. The input data and output data are then recorded by the signal analyzer. The aforementioned

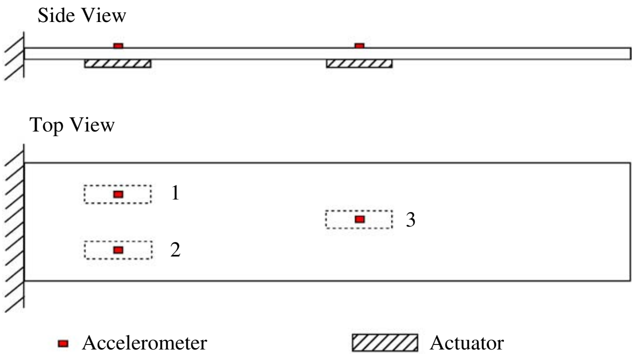

Fig. 9. The piezoelectric structure considered in experimental investigation.

(a)

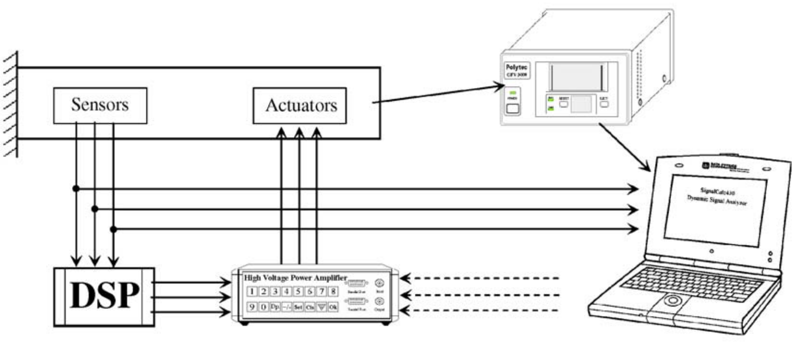

(b)

Fig. 10. The experimental setup: (a) picture of the overall experimental setup; (b) schematic diagram of the experimental setup.

identification procedure is employed to set up the corresponding state space model. The LQG controller is designed and then coded into the DSP. The free parameters of the LQG controller are determined based on engineering judgement through an iterative procedure. The active vibration control system is schematically shown in Fig. 10(b). Firstly, the acceleration signals monitored by the three accelerometers are put into the digital control system, which is built on the DSP board. Proper control signals generated by the control

Table 2
Natural frequencies of the structure

Mode	Natural frequency (Hz)
1	4.44
2	26.56
3	71.92
4	139.65

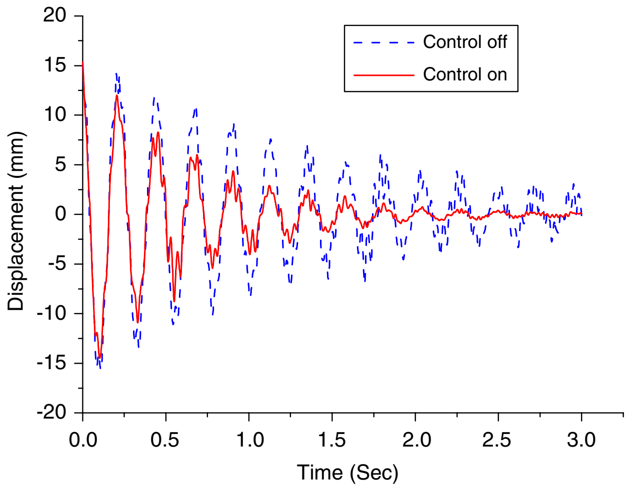

Fig. 11. Transient response of the plate due to initial tip displacement.

program according to the control law are then amplified by the high voltage amplifier and fed back to the piezoelectric patches to perform closed loop control of the structure. The experimental results presented in this study are limited to the case in which the vibration of the structure is generated by an initial displacement of 15 mm. Fig. 11 shows the open loop and closed loop dynamic displacement response of the plate at the free end monitored by the Polytec OFV-3000 laser vibrometer. As can be seen from Fig. 11, the vibration is well suppressed by using the controller.

5. Conclusions

Under the interaction of structure and control disciplines, a general scheme of analyzing and designing piezoelectric smart structures is successfully developed in this study. The scheme involves using a modern system identification technique known as OKID approach to develop an equivalent linear model from the outputs of the commercial finite element code ANSYS. Standard control law design techniques are then used to design control laws. By using APDL, the resulting control laws are then incorporated into transient analysis for evaluation. Numerical results are presented to demonstrate the efficiency of the proposed scheme in simulating an actively controlled piezoelectric structure. It is pertinent to mention that the proposed design scheme can further reduce cost, as well as shorten design cycle time for smart structures. Further more, the proposed scheme can integrate a user selected control algorithm into the ANSYS finite element model to perform closed loop simulation. Unfortunately, the application of the proposed scheme is limited to piezoelectric smart structures. As to other smart structures, such as smart structures using shape memory alloys or fiber optics, the scheme can't be applied successfully.

Finally, a complete active vibration control system comprising the cantilever plate, the piezoelectric actuators, the accelerometer and the DSP board is then set up to conduct experimental investigation. System identification technique is employed to establish the state space model of the physical system before conducting the vibration control experiment. This method is considered to be more universal than analytical or numerical methods, especially for complex systems, in which analytical solutions are impractical, if not impossible. From the experimental results, it is observed that satisfactory performance of vibration attenuation can be achieved. The feasibility of OKID approach in the vibration control of piezoelectric smart structures is verified successfully. Equivalent linear models developed by employing OKID approach can represent the physical system very well.

Acknowledgements

This work was supported by the National Natural Science Foundation of China (NSFC) under Grant no. 50390063 and the foundation of National Key Laboratory of defense technology under Grant no. 51463040403JW0301. The authors also gratefully acknowledge the helpful suggestion of the reviewers.

References

[1] X.Q. Peng, K.L. Lam, G.R. Liu, Active vibration control of composite beams with piezoelectrics: a finite element model with third order theory, *Journal of Sound and Vibration* 209 (4) (1998) 635–650.
[2] K. Ma, Adaptive nonlinear control of a clamped rectangular plate with PZT patches, *Journal of Sound and Vibration* 264 (4) (2003) 835–850.
[3] K. Ma, M.N. Ghasemi-Nejhad, Frequency-weighted adaptive control for simultaneous precision positioning and vibration suppression of smart structures, *Smart Materials and Structures* 13 (5) (2004) 1143–1154.
[4] M. Sunar, S.S. Rao, Recent advances in sensing and control of flexible structures via piezoelectric materials technology, *Applied Mechanics Reviews* 52 (1) (1999) 1–16.
[5] A. Benjeddou, Advances in piezoelectric finite element modeling of adaptive structural elements: a survey, *Computers and Structures* 76 (1-3) (2000) 347–363.
[6] J. Mackerle, Smart materials and structures-a finite-element approach: a bibliography (1986–1997), *Modelling and Simulation in Materials Science and Engineering* 6 (3) (1998) 293–334.
[7] J. Mackerle, Smart materials and structures—a finite element approach—an addendum: a bibliography (1997–2002), *Modelling and Simulation in Materials Science and Engineering* 11 (5) (2003) 707–744.
[8] S.X. Xu, T.S. Koko, Finite element analysis and design of actively controlled piezoelectric smart structures, *Finite Element in Analysis and Design* 40 (3) (2004) 241–262.
[9] C.P. Smyser, K. Chandrashekhara, Robust vibration control of composite beams using piezoelectric devices and neural networks, *Smart Materials and Structures* 6 (2) (1997) 178–189.
[10] C. Hwu, W.C. Chang, H.S. Gai, Vibration suppression of composite sandwich beams, *Journal of Sound and Vibration* 272 (1) (2004) 1–20.
[11] J.-N. Juang, M. Phan, *Identification and control of mechanical systems*, Cambridge University Press, New York, 2001.
[12] J.-N. Juang, M. Phan, Lucas G. Horta, Identification of observer/Kalman filter Markov parameters: theory and experiments, *Journal of Guidance, Control and Dynamics* 16 (2) (1993) 320–329.
[13] J.-N. Juang, R.S. Pappa, An eigensystem realization algorithm for modal parameter identification and model reduction, *Journal of Guidance, Control and Dynamics* 8 (5) (1985) 620–627.
[14] M.V. Gandhi, B.S. Thompson, *Smart Materials and Structures*, Chapman & Hall, London, 1992.
[15] S. Narayanan, V. Balamurugan, Finite element modelling of piezolaminated smart structures for active vibration control with distributed sensors and actuators, *Journal of sound and vibration* 262 (3) (2003) 529–562.
[16] A. Zallo, P. Gaudenzi, Finite element models for laminated shells with actuation capability, *Composite and Structures* 81 (8-11) (2003) 1059–1069.
[17] K.J. Bathe, *Finite Element Procedures*, Prentice-Hall, Englewood Cliffs, NJ, 1996.
[18] M. Scott, M. Gilbert, M. Demeo, Active vibration Damping of the space shuttle remote manipulator system, *Journal of Guidance, Control and Dynamics* 16 (2) (1993) 275–280.
[19] M. Phan, L.G. Horta, J.-N. Juang, et al., Linear system identification via an asymptotically stable observer, *Journal of optimization and applications* 79 (1) (1993) 59–86.
[20] F. Lewis, V.L. Syrmos, *Optimal Control*, Wiley, New York, 1995.
[21] L. Ljung, *System Identification: Theory for the User*, Prentice-Hall, Englewood Cliffs, NJ, 1987.